Origin of the Damping Effect on the Stereoselectivity of Electrophile Capture Caused by the Remote Double Bond in Lithium Tricyclo[5.2.1.$0^{2,6}$]deca-3,5,8-trienide. Structure of This Cyclopentadienide in Tetrahydrofuran Solution

Leo A. Paquette,*,† Mark R. Sivik,†,[1] Walter Bauer,*,‡ and Paul von Ragué Schleyer‡

Evans Chemical Laboratories, The Ohio State University, Columbus, Ohio 43210, and Institut für Organische Chemie der Universität Erlangen-Nürnberg, Henkestrasse 42, D-91054 Erlangen, Germany

Received May 5, 1994®

The stereochemical course of the reaction of lithium tricyclo[5.2.1.$0^{2,6}$]deca-3,5,8-trienide (**3**) with $BrCH_2CD_2Cl$, chlorotrimethylsilane, and ferrous chloride has been defined. While essentially no facial discrimination was seen during the spirocyclopropane ring closure, the exo isomer predominated slightly in the silylation product mixture. The distribution of ferrocenes was 56% exo/exo, 38% exo/endo, and 6% endo/endo. Multinuclear NMR studies (^1H, ^{13}C, ^6Li) have shown the title compound **3** to exist as a monomer at rt (room temperature) and as a dimer–monomer pair (0.7:1) at −108 °C. ^1H HOESY (heteronuclear Overhauser effect) spectroscopy (using ^6Li) showed the lithium cation to be located at the endo face in the monomer and at the two endo faces in the dimer. High-field shifts are observed in the ^6Li spectrum: $\delta = -7.12$ (monomer) and $\delta = -11.68$ (sandwiched Li in the dimer) due to ring current shielding. MNDO calculations on **3** show the endo,endo dimer to be more stable than the exo,exo dimer in agreement with experiment. While, in modest contradiction to observations, MNDO indicates the exo monomer to be slightly more stable than its endo isomer, it does show the trend towards greater endo stability in **3**(**23**) due to the presence of the CC double bond.

Introduction

Tricyclo[5.2.1.$0^{2,6}$]deca-2,5,8-triene (**1**) enters into Diels–Alder reactions with methyl acrylate,[2] methyl propiolate,[2] maleic anhydride,[2] *p*-benzoquinone,[2] benzyne,[2] *N*-methyltriazolinedione,[3] singlet oxygen,[4] and (*Z*)-1,2-bis(phenylsulfonyl)ethylene[5] to give the corresponding endo adduct predominantly or exclusively.[6] This remarkable stereochemical preference parallels very closely the response[7] exhibited by isodicyclopentadiene (**2**), its dihydro counterpart, although **1** generally exhibits lower reactivity.[8] This kinetic retardation is quite possibly a reflection of the electron-withdrawing inductive contributions of the norbornenyl π-bond in **1**.

1 **2**

A limited number of experiments indicate that the additional unsaturation in the corresponding lithium cyclopentadienide **3** has considerably greater influence

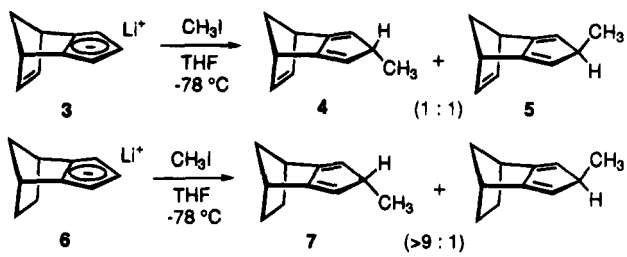

on the stereoselectivity of electrophilic capture relative to **6**. For example, the alkylation of **3** with methyl iodide in THF at −78 °C afforded a 1:1 mixture of **4** and **5**.[9] Comparable treatment of **6** leads predominantly to the formation of **7**. The face selectivity exhibited by **6** is

† The Ohio State University.
‡ Universität Erlangen-Nürnberg.
® Abstract published in *Advance ACS Abstracts,* November 1, 1994.

(1) National Need Fellow, 1989, 1990. Amoco Foundation Fellow, 1991.

(2) (a) Paquette, L. A.; Carr, R. V. C.; Böhm, M. C.; Gleiter, R. *J. Am. Chem. Soc.* **1980**, *102*, 1186. (b) Böhm, M. C.; Carr, R. V. C.; Gleiter, R.; Paquette, L. A. *J. Am. Chem. Soc.* **1980**, *102*, 7218.

(3) Paquette, L. A.; Carr, R. V. C.; Charumilind, P.; Blount, J. F. *J. Org. Chem.* **1980**, *45*, 4907.

(4) Hathaway, S. J.; Paquette, L. A. *Tetrahedron* **1985**, *41*, 2037.

(5) (a) Paquette, L. A.; Künzer, H.; Green, K. E. *J. Am. Chem. Soc.* **1985**, *107*, 4788. (b) Paquette, L. A.; Künzer, H.; Green, K. E.; DeLucchi, O.; Licini, G.; Pasquato, L.; Valle, G. *J. Am. Chem. Soc.* **1986**, *108*, 3453.

(6) Reviews: (a) Paquette, L. A. In *Stereochemistry and Reactivity of Pi Systems*; Watson, W. H., Ed.; Verlag Chemie International: Deerfield Beach, FL, 1983, pp 41–73. (b) Gleiter, R.; Paquette, L. A. *Acc. Chem. Res.* **1983**, *16*, 328.

(7) Triazolinediones (both *N*-methyl and *N*-phenyl) behave exceptionally. Whereas **1** exhibits complete endo stereoselectivity in the (4 + 2)π cycloadditions to these dienophiles, **2** is entirely exo-selective: Paquette, L. A.; Green, K. E.; Hsu, L.-Y. *J. Org. Chem.* **1984**, *49*, 3650.

(8) Paquette, L. A.; Hayes, P. C.; Charumilind, P.; Böhm, M. C.; Gleiter, R.; Blount, J. F. *J. Am. Chem. Soc.* **1983**, *105*, 3148. Specifically, kinetic studies were carried out with dimethyl acetylenedicarboxylate as the dienophile.

(9) Paquette, L. A.; Charumilind, P.; Kravetz, T. M.; Böhm, M. C.; Gleiter, R. *J. Am. Chem. Soc.* **1983**, *105*, 3126.

0276-7333/94/2313-4919$04.50/0

recognized to be temperature-sensitive; exo attack is preferred at 20–25 °C.[10,11] This crossover is consistent with the varied manner in which the lithium counterion is complexed to **6** in THF solution at different temperatures.[12] Near −78 °C, a monomer–dimer equilibrium can be observed spectroscopically. Presumably, the peripheral, nonsandwiched Li^+ in the more reactive **8**

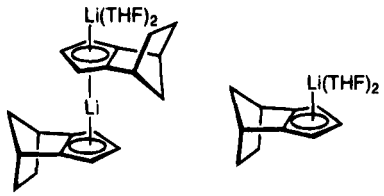

8 **9**

attracts the electrophile to the endo face where subsequent C–C bond formation occurs with retention of configuration. At room temperature, the prevailing exo monomer **9** behaves analogously, the assumption again being that the retention transition state is of lower energy than that resulting in inverted product.

Herein we describe the capture of **3** with additional electrophiles of rather divergent type as well as NMR and MNDO studies of this lithium salt in THF solution.[13] The combination of experimental and computational results provide a coherent rationale for the reduced capacity of **3** to achieve high levels of facial stereoselectivity.

Results

Electrophilic Capture Experiments. A second carbon–carbon bond-forming reaction involving **3** was investigated first. The dry, powdery lithium salt was dissolved in anhydrous THF, cooled to 0 °C, and treated with $BrCH_2CD_2Cl$. The initial nucleophilic displacement was expected on the basis of precedent (Br/Cl ≈ 50)[14] to occur at the nondeuterated carbon of the electrophile to give a stereoisomeric mixture of the two chloroethylated products. Since the ultimate goal was to advance to the spirocyclopropane derivatives, the stereochemical course of this first step was not elucidated. Nor was it considered to be linked to the outcome of the second stage since a common cyclopentadienide results upon deprotonation of either diastereomer. For standardization purposes, the proton abstraction was performed at −78 °C with a lithium base, viz., the bis(trimethylsilyl)amide. Although a mixture of **10** and **11** was produced under these conditions, neither NOE techniques nor ^2H NMR methods could be used to deduce the relative proportion of the two isomers because of our inability to define the respective cyclo-

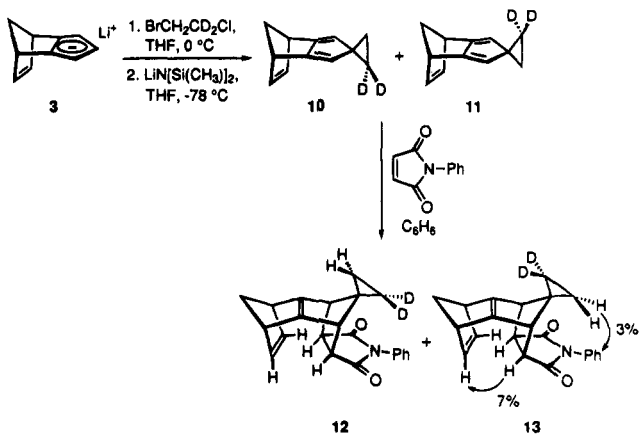

3 **10** **11** **12** **13**

propyl shifts unambiguously. Consequently, the spirocyclopropane mixture was converted to **12** and **13** by condensation with *N*-phenylmaleimide. NOE on these adducts (see **13** for example) indicated a 48:52 ratio of **12** to **13**. Consequently, there is essentially no facial discrimination during the cyclopropane ring closure step.

In another series of experiments, **3** was exposed to chlorotrimethylsilane in THF at −78 °C. The resulting silanes **14** and **15** proved to be separable by preparative

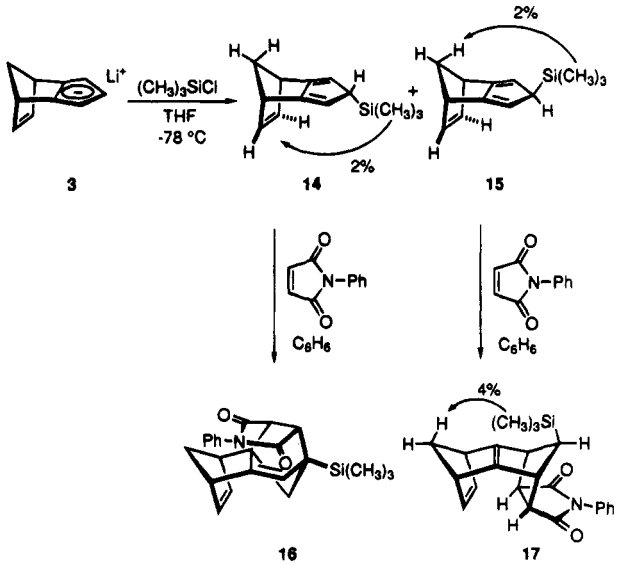

3 **14** **15** **16** **17**

HPLC. Tentative stereochemical assignments were made on the basis of long-range NOE effects (see drawings). On this basis, exo isomer **15** predominated slightly in the mixture (ratio 47:53). Further corroboration of the relative configurations was gained as before by Diels–Alder cycloaddition to *N*-phenylmaleimide in benzene at room tempera-ture. Silane **15** behaved as expected, providing **17**. The level of NOE interaction between the Me_3Si protons and the syn proton of the neighboring methano bridge confirmed both the original stereochemical assignment and the endo direction of dienophile approach. Endo isomer **14** did not behave analogously, undergoing instead kinetically favored 1,5-silatropic shift prior to (4 + 2) capture of the dienophile.[10] This pre-cycloaddition event ultimately leads to the formation of **16** with loss of information regarding the stereogenicity of the carbon atom originally bonded to silicon. Nonetheless, the weight of cumulative evidence requires that **14** be the endo isomer.

(10) Paquette, L. A.; Charumilind, P.; Gallucci, J. C. *J. Am. Chem. Soc.* **1983**, *105*, 7364.
(11) (a) Paquette, L. A.; Moriarty, K. J.; Meunier, P.; Gautheron, B.; Crocq, V. *Organometallics* **1988**, *7*, 1873. (b) Paquette, L. A.; Moriarty, K. J.; Meunier, P.; Gautheron, B.; Sornay, C.; Rogers, R. D.; Rheingold, A. L. *Organometallics* **1989**, *8*, 2159.
(12) Paquette, L. A.; Bauer, W.; Sivik, M. R.; Bühl, M.; Feigel, M.; Schleyer, P. v. R. *J. Am. Chem. Soc.* **1990**, *112*, 8776.
(13) For similar studies on structurally related systems (although lacking a distal double bond), see: (a) Bauer, W.; O'Doherty, G. A.; Schleyer, P. v. R.; Paquette, L. A. *J. Am. Chem. Soc.* **1991**, *113*, 7093. (b) Bauer, W.; Sivik, M. R.; Friedrich, D.; Schleyer, P. v. R.; Paquette, L. A. *Organometallics* **1992**, *11*, 4178.
(14) This is an average value for intermolecular S_N2 displacement reactions: Streitwieser, A., Jr. *Solvolytic Displacement Reactions*; McGraw-Hill: New York, 1962; p 30 (*Chem. Rev.* **1956**, *56*, 571).

Attempts were subsequently made to condense **3** with $TiCl_3$, $CpTiCl_3$, $MeCpTiCl_3$, and $CpZrCl_3$ as representative organometallic electrophiles. Unfortunately, complex reaction mixtures resulted in each instance and chromatographic separation was not readily feasible for these reactive products. Pure group 4 metal complexes of **1** can readily be prepared by exposure of the individual silanes with reactive Ti and Zr chlorides.[15] The example shown involves the treatment of **14** with $TiCl_4$

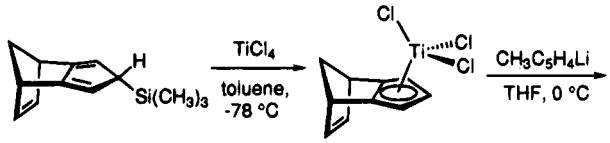

14 **18**

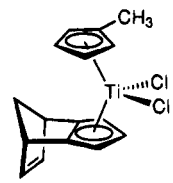

19

in cold toluene to give **18** (73%) and further reaction of this stereoinverted complex with the MeCp anion. Although **19** is obtained as a stereochemically homogeneous substance (66%), its acquisition provides no direct information on issues relevant to the present investigation.

For this reason, a THF solution of **3** was added to a slurry of $FeCl_2$ in the same solvent at −78 °C. Analysis of the unpurified reaction mixture by high-field ^1H NMR showed three ferrocenes to have formed in the ratio of 56:38:6. Dissolution of this oil in a minimal amount of hexane and cooling to −20 °C permitted isolation of the major complex, a yellow solid, identified as the exo,exo isomer **20**. This substance had been described earlier[16]

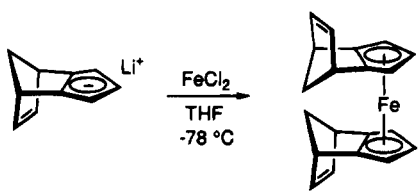

3 **20**

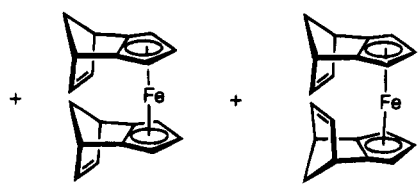

21 **22**

and its electrochemical behavior examined more recently.[17] No further effort was expended to achieve the separation of **21** from **22**.[18] However, the telltale chemical shifts of their etheno protons (δ 6.61 and 6.57 for **21** and δ 6.31 for **22** in C_6D_6 solution) allowed for their ready identification in the mixture.

^1H and ^{13}C NMR Spectra at Room Temperature. For the NMR studies involving **3**, material enriched with the ^6Li isotope (96%) was employed. The merits of ^6Li (spin I = 1, natural abundance 7.4%) over the major isotope ^7Li (spin $I = {}^3/_2$, natural abundance 92.6%) are well documented.[19] For convenience, the numbering and nomenclature shown in structure **23** has been used.

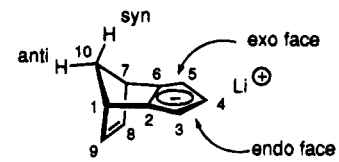

23 ≡ 3

At +26 °C, a THF-d_8 solution of **3**(≡**23**) exhibits a single set of signals both in the ^1H and the ^{13}C spectrum. Similar observations have been made for numerous other organolithium compounds. Thus, we deal either with a single species of **3** in THF at rt (room temperature) or with two or more rapidly exchanging species.

The assignment of proton resonances H1···H9 in **3**(**23**) is straightforward (cf. Figure 1). However, the assignment of those resonances due to H10(anti) and H10(syn) at δ = 2.32 and 2.07 ppm is less trivial. Since their proper assignment is of crucial importance for locating the associated counterion (see below), a two site approach was under-taken. Unfortunately, no additional W-type coupling was observed in the AB spectrum of H10(anti) and H10(syn) as a means of facilitating the interpretation.[20] In principle, a difference NOE spectrum should exhibit dipolar interactions between H10(anti) and H8,9, as well as between H10(syn) and H3,4,5. However, continuous wave irradiation of H10(anti) and H10(syn) led to *negative* NOEs at rt in THF-d_8 for *all* of the protons in **3**(**23**). This phenomenon is known as "spin diffusion" and is usually observed in cases of slowly tumbling molecules, with $\omega\tau < 1$ (where ω is the proton Larmor frequency, and τ is the molecular correlation time).[21]

In contrast to such NOE experiments, rotating frame experiments (ROEs) permit the detection of positive NOEs even for slowly reorienting molecules.[21] We have carried out a selective 1D-ROE difference experiment for **3**(**23**).[22] The pulse sequence of this method is shown in eq 1. FID1 and FID2 are subsequently subtracted,

(15) (a) Cordoso, A. M.; Clark, R. J. H.; Moorhouse, S. *J. Chem. Soc., Dalton Trans.* **1980**, 1156. (b) Sornay, C.; Gautheron, B.; O'Doherty, G. A.; Paquette, L. A. *Organometallics* **1991**, *10*, 2082. (c) Paquette, L. A.; Sivik, M. R. *Organometallics* **1992**, *11*, 3503.

(16) (a) Hsu, L.-Y.; Hathaway, S. J.; Paquette, L. A. *Tetrahedron Lett.* **1984**, 259. (b) Paquette, L. A.; Schirch, P. F. T.; Hathaway, S. J.; Hsu, L.-Y.; Gallucci, J. C. *Organometallics* **1986**, *5*, 490.

(17) Gallucci, J. C.; Opromolla, G.; Paquette, L. A.; Pardi, L.; Schirch, P. F. T.; Sivik, M. R.; Zanello, P. *Inorg. Chem.* **1993**, *32*, 2292.

(18) Bhide, V.; Rinaldi, P.; Farona, M. F. *J. Organomet. Chem.* **1989**, *376*, 91.

(19) (a) Bauer, W.; Schleyer, P. v. R. In *Advances in Carbanion Chemistry;* Snieckus, V., Ed.; Jai Press: Greenwich, CT, 1992; Vol. 1, p 89. (b) Günther, H.; Moskau, D.; Schmalz, D. *Angew. Chem.* **1987**, *99*, 1242. *Angew. Chem., Int. Ed. Engl.* **1987**, *26*, 1212. (c) Thomas, R. D. In *Isotopes in the Physical and Biomedical Sciences: Isotope Applications in NMR Studies*; Buncel, E., Jones, J. R., Eds.; Elsevier: Amsterdam, 1992; p 367. (d) Fraenkel, G.; Hsu, H.; Su, B. M. In *Lithium: Current Applications in Science, Medicine, and Technology*; Bach, R. O., Ed.; J. Wiley: New York, 1985. (e) Bauer, W. In *Lithium Compounds: Principles and Applications*; Sapse, A.-M., Schleyer, P. v. R., Eds.; Wiley: New York, in press.

(20) Marchand, A. P. *Stereochemical Applications of NMR Studies in Rigid Bicyclic Systems;* VCH: Deerfield Beach, FL, 1982.

(21) Neuhaus, D.; Williamson, M. *The Nuclear Overhauser Effect in Structural and Conformational Analysis*; VCH Publishers: New York, 1989.

(22) Kessler, H.; Oschkinat, H.; Griesinger, C.; Bermel, W. *J. Magn. Reson.* **1986**, *70*, 106.

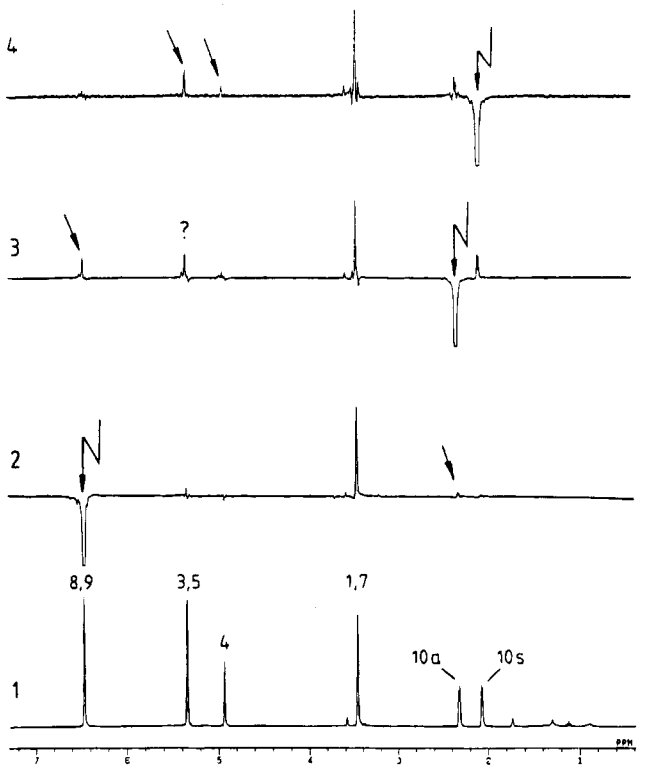

Figure 1. 1D-ROE difference spectrum of **3(23)**, 1 M in THF-d_8, +26 °C, pulse sequence (1), spin lock time 0.7 s. For the assignment numbers, see formula **3(23)**; a = anti; s = syn. Flash arrows indicate the sites of the selective 180° inversion pulses. Normal arrows indicate positive ROEs. ? = ROE of unknown origin; see text. Trace no. 1 is a normal 1D spectrum.

delay−180°(soft, on res.)−90°(hard)−spin lock−
FID1−delay−180°(soft, off res.)−90°(hard)−
spin lock−FID2 (1)

resulting in signal enhancement for nuclei spatially close to the selectively irradiated nucleus. Figure 1 shows the result of the 1D ROE difference experiment applied to **3(23)**.

Selective population inversion of olefinic protons H8,9 results in an enhancement of the signal at δ = 2.32 (trace no. 2), thereby identifying this resonance to be due to H10 (anti). Likewise, selective inversion of the δ = 2.32 signal yields a significant enhance-ment of the resonance due to H8,9 (trace no. 3). By contrast, irradiation at δ = 2.07 results in no H8,9 signal intensity increase. Instead, the resonances of the Cp ring protons H3,4,5 are enhanced. Thus, the signal at δ = 2.07 must be due to H10 (syn) (trace no. 4).

In trace no. 3 of Figure 1, an additional signal enhancement is observed for H3,5 which does not match the assignment of δ = 2.32 as H10 (anti). The origin of this signal is not clear. In order to corroborate the correct H10(anti)/H10(syn) assignment unequivocally, heteronuclear NOE was employed to detect close proximities between heteronuclei, e.g. ^{13}C and ^{1}H. A 2D NMR variant, termed "heteronuclear Overhauser effect spectroscopy" (HOESY) permits the detection of a large number of such dipolar interactions in a single experiment.[23] The basic HOESY pulse sequence is given in

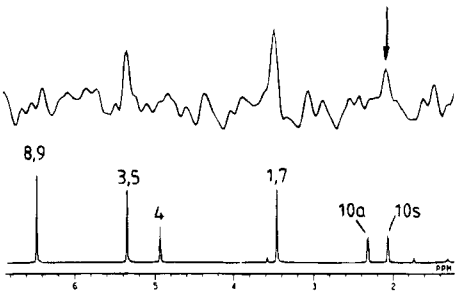

Figure 2. ^{13}C, ^{1}H HOESY spectrum of **3(23)** (1 M in THF-d_8, +26 °C), recorded with the pulse sequence (3) proposed by Bigler. Only the f_1 cross section at the chemical shift of C2,6 is shown (top) along with the one-dimensional ^{1}H spectrum (bottom). For the assignment numbers, see formula **3(23)**; a = anti; s = syn. The arrow indicates a cross peak between C2,6 and H10(syn).

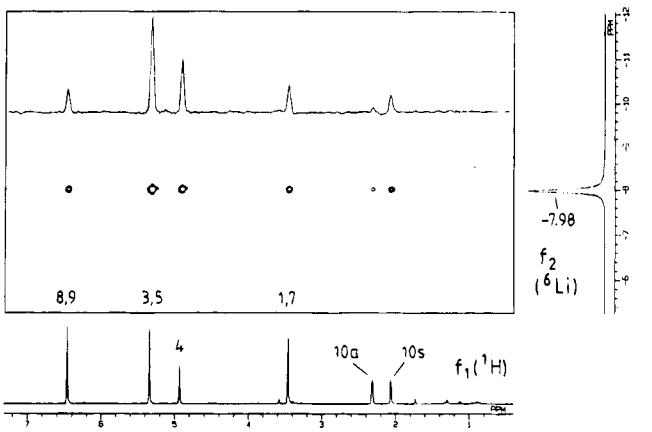

Figure 3. Phase-sensitive ^{6}Li,^{1}H HOESY spectrum of **3(23)**, 1 M in THF-d_8, +26 °C, mixing time 2.0 s. The inset shows the f_1 cross section cut at δ(Li) = −7.98 ppm. For the assignment numbers, see formula **3(23)**; a = anti; s = syn.

eq 2. An improvement in the basic pulse sequence has

90°(I)−t_1/2−180°(S)−t_1/2−90°(I)−τ_m−90°(S)−
FID/BB−decoupl. (2)

(180°(S)−90°(I)−t_1/2−180°(S)−t_1/2−90°(I)−τ_m)$_n$−
90°(S)−FID/BB−decoupl. (3)

been described by Bigler.[24] Repeated looping through the preparation, evolution, and mixing period leads to an increase in the cross peak intensity. The pulse sequence is given in eq 3. Use will also be made below of HOESY in two dimensional ^{6}Li,^{1}H NMR experiments.

In order to unequivocally assign H10(anti) and H10-(syn) of **3(23)** at rt, a 2D-^{13}C,^{1}H HOESY experiment with the Bigler modification was performed according to eq 3. The proximity between H10(syn) and carbon atoms C2,6 of the Cp ring in **3(23)** should manifest itself in cross peaks between the appropriate ^{1}H and ^{13}C resonances. Figure 2 shows an f_1 cross section of a ^{13}C, ^{1}H HOESY spectrum performed on **3(23)** at rt and cut at the chemical shift of C2,6. Expectedly, cross peaks are observed which involve protons 1,7 and 3,5. In addition, a cross peak at the high-field resonance of the H10 syn/anti pair assigns this resonance to be due to H10(syn).

(23) (a) Rinaldi, P. L. *J. Am. Chem. Soc.* **1983**, *105*, 5167. (b) Yu, C.; Levy, G. C. *J. Am. Chem. Soc.* **1983**, *105*, 6994.

(24) (a) Bigler, P. *Helv. Chim. Acta* **1988**, *71*, 446. (b) Bigler, P.; Müller, C. *J. Magn. Reson.* **1988**, *79*, 45.

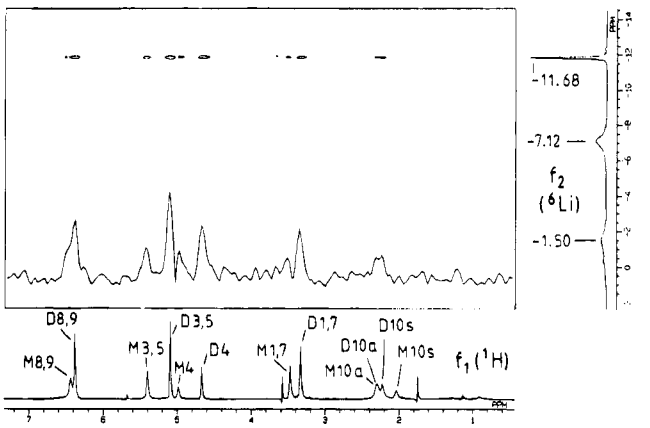

Figure 4. Magnitude mode ^{6}Li, ^{1}H HOESY spectrum of **3(23)** in THF-d_8, 1 M, −108 °C, mixing time 2.0 s. The inset shows the f_1 cross section cut at δ(Li) = −11.68 ppm. For the assignment numbers, see formula **3(23)**. D = dimer **27**; M = monomer **28**; a = anti; s = syn.

Table 1. ^{1}H Chemical Shifts of 3(23) at +26 °C and Isomers 27 and 28 at −109 °C (1.0 M, THF-d_8)

		−109 °C	
H	+26 °C **3(23)**	endo monomer **28**	endo, endo dimer **27**
1,7	3.46 (s)	3.47	3.33
3,5	5.34 (d, 2.8 Hz)	5.39	5.08
4	4.93 (t, 2.8 Hz)	4.98	4.65
8,9	6.46 (s)	6.37	6.37
10(syn)	2.07 (d, 5.4 Hz)	2.03	2.22
10(anti)	2.32 (d, 5.4 Hz)	2.29	2.29

^{1}H and ^{13}C NMR Spectra at Low Temperature. At −100 °C, two signal sets are observed for a 1.0 M solution of **3(23)** in THF-d_8, both in the ^{1}H and ^{13}C NMR spectrum (cf. Figure 4). Similar observations have been made for isodiCpLi (**6**) in the same solvent.[12] A detailed study[12] of **6** revealed these two species to be exo,exo dimer **8** and exo monomer **9**. By analogy, we conclude that a similar monomer−dimer equilibrium exists in **3(23)**. In the following, the location of lithium in these two forms is identified.

By analogy to **6**, the lower field Cp ring ^{1}H signals (5.39 and 4.98 ppm) are assigned to the monomer and the analogous high-field signals (5.08 and 4.65 ppm) to the dimer (cf. Table 1). Integration as well as weighing of the signal cutouts yields a dimer:monomer ratio of 0.7:1. The same relationship (dimer signal at higher field than the monomer signal) also holds for the resonance due to H1,7.

In both the monomer and the dimer of **3(23)**, the chemical shift of H10(syn) is *upfield* from the corresponding H10(anti) chemical shift. H10(syn) lies partly in the shielding cone of the Cp ring, thus experiencing the effect of magnetic anisotropy (ring current). By contrast, in **6** the chemical shift order for H10 (anti/syn) is reversed. The shielding effect of the Cp ring is counteracted by the electric field produced by lithium on the exo face of **6**. The proximity of lithium to a proton has been found to exert a downfield shift in the ^{1}H spectrum.[25] From the missing downfield shift observed for the two forms of **3(23)** at low temperature, lithium is deduced to be located *endo* in both the monomer and the dimer. This conclusion will be corroborated by further observations below.

Table 2. ^{13}C Chemical Shifts of 3(23) at +26 °C and Isomers 27 and 28 at −109 °C (1.0 M, THF-d_8)

		−109 °C	
C	+26 °C **3(23)**	endo monomer **28**	endo, endo dimer **27**
1,7	47.20	47.44	47.15
2,6	131.47	130.32	129.97
3,5	98.49	97.53	98.06
4	98.53	99.60	99.23
8,9	143.71	143.54	144.02
10	71.24	69.77	70.77

A similar situation has been found in the camphor-derived CCpLi (**24**). Here, the resonance of methyl group 13 in endo,endo dimer **25** resonates at appreciably higher field than its analog in exo monomer **26**.[13] Hence, the endo,endo dimer **27** and the endo monomer **28** are the two forms of **3(23)** present at low temperature.

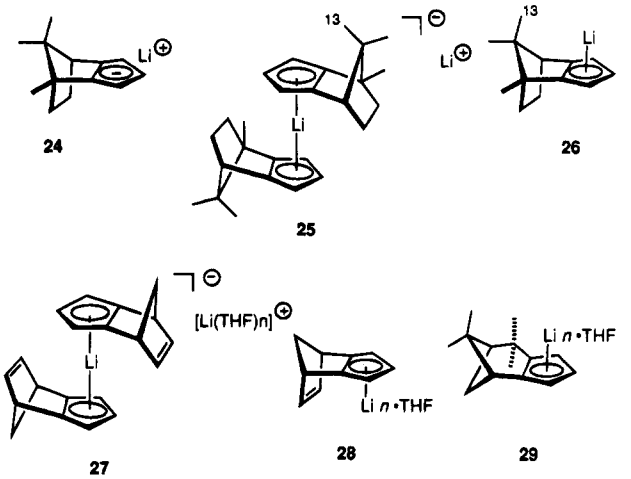

Tables 1 and 2 show the ^{1}H and ^{13}C chemical shifts of **27** and **28** observed at low temperature, as well as the chemical shifts of their structural counterpart **3(23)** observed at room temperature. The ^{1}H chemical shifts of the room temperature species closely resemble those of the low-temperature monomer **28** and differ considerably from those of the low-temperature dimer **27**. Hence, the endo lithio monomer **28** is being observed exclusively or nearly exclusively at rt. Again, this resembles the behavior of isodiCpLi (**6**) where at low temperature a dimer−monomer equilibrium is found and only monomer is present at room temperature. This implies that the monomer−dimer equilibrium of **3(23)** must be exothermic ($\Delta H° < 0$).

^{6}Li NMR Spectra. At rt, **3(23)**shows a single ^{6}Li resonance in THF solution. The chemical shift (δ = −7.98) is outside the "normal" range of −2 to +2 ppm. Such unusual upfield shifts have been observed for isodiCpLi (**6**),[12] CCpLi (**24**),[13a] and the verbenone-derived compound **29**.[13b] Ring current effects are responsible for this phenomenon.

Spatial proximities between ^{6}Li and protons may be detected by using ^{6}Li, ^{1}H HOESY (heteronuclear Overhauser effect spectroscopy).[12,13,25-27] This technique allows proper differentiation between the exo or endo location of lithium in **3(23)**.

(25) Bauer, W.; Schleyer, P. v. R. *J. Am. Chem. Soc.* **1989**, *111*, 7191. Bauer, W.; Feigel, M.; Müller, G.; Schleyer, P. v. R. *J. Am. Chem. Soc.* **1988**, *110*, 6023. Bauer, W.; Winchester, W. R.; Schleyer, P. v. R. *Organometallics* **1987**, *6*, 2371. Bauer, W.; Clark, T.; Schleyer, P. v. R. *J. Am. Chem. Soc.* **1987**, *109*, 970.

Table 3. MNDO-Calculated Distances between Lithium and Individual H-Positions in 3(23), Calculated for Disolvated (Me_2O) Species

H	exo-Li	endo-Li
1,7	4.10	4.31
3,5	3.11	3.11
4	3.04	3.04
8,9	5.53	4.18
10(anti)	4.72	5.33
10(syn)	3.23	4.75

Figure 3 shows the ^{6}Li, ^{1}H HOESY spectrum obtained for **3(23)**at rt. Intense cross peaks indicate tight contact between lithium and the anion moiety. As was the case for **6**, **24**, and **29**, the most intense cross peaks are detected between the lithium signal and the Cp proton resonances, indicating that the lithium ion is located at the exo or the endo face of the Cp ring. The cross peak at the H1,7 chemical shift does not differentiate between exo or endo lithium. The f_1 cross section in the box in Figure 3 demonstrates that the H10(syn) and H8,9 cross peaks are of comparable intensity, indicating that the Li–H10(syn) and Li–H8,9 distances must not differ much. Hence, the endo orientation of lithium is exclusive or nearly so.

Table 3 shows internuclear distances between lithium and the individual H positions in exo and endo **3(23)** as obtained by MNDO calculations. In the exo lithio isomer, the separation (5.53 Å) between Li and H8,9 is the largest in the data set. Hence, the Li–H8,9 cross peak involved should be vanishingly small. By contrast, the distance between Li and H10(syn) is nearly identical to the separation between Li and the Cp ring protons. This can be expected to result in a very intense cross peak. Clearly, this is not observed in Figure 3. Hence, the exo isomer must not be present. In contrast, the MNDO distances involved in the endo Li isomer are of comparable magnitude, in agreement with results in the Figure 3 spectrum.

At −108 °C, three ^{6}Li signals at δ = −1.50, −7.12, and −11.68 ppm are seen (cf. Figure 4). This is similar to the observations made for isodiCpLi (**6**)[12] and is interpreted to be due to a monomer–dimer equilibrium. Monomer bound lithium resonates at δ = −7.12 ppm whereas the "sandwiched" lithium in the dimer experiences a 2-fold ring current induced high-field shift (δ = −11.68 ppm). The $Li(THF)_n^+$ counterion in the dimer, which is presumably peripherally bound to the dimer anion (cf. Chart 1) resonates at δ = −1.50 ppm. The associated exchange mechanisms must be similar to those found for isodiCpLi (**6**). Likewise, the exchange rates in **3(23)** must be of an order comparable to those found for isodiCpLi (**6**). The exchange between monomer-bound lithium and $Li(THF)_n^+$ is still rapid at −108 °C and broadened signals not far from coalescence are obtained.

Figure 4 shows the ^{6}Li,^{1}H HOESY spectrum obtained for **3(23)** at −108 °C. Due to the broadness of the δ = −7.12 and −1.50 peak, detectable cross peaks are obtained only for the sharp dimer signal at δ = −11.68. Due to the appreciable chemical exchange rate observed even at −108 °C, magnetization transfer takes place during the mixing time of the pulse sequence. Thus, cross peaks are observed for the Li peak at δ = −11.68 ppm both with the dimer and with the monomer ^{1}H resonances. Apart from the "expected" cross peaks at H1,7 and H3,4,5, an intense cross peak is observed for H8,9 and a smaller cross peak for H10(syn). This indicates an endo-oriented lithium for the same reasons outlined above for the room-temperature species. Thus,

Chart 1

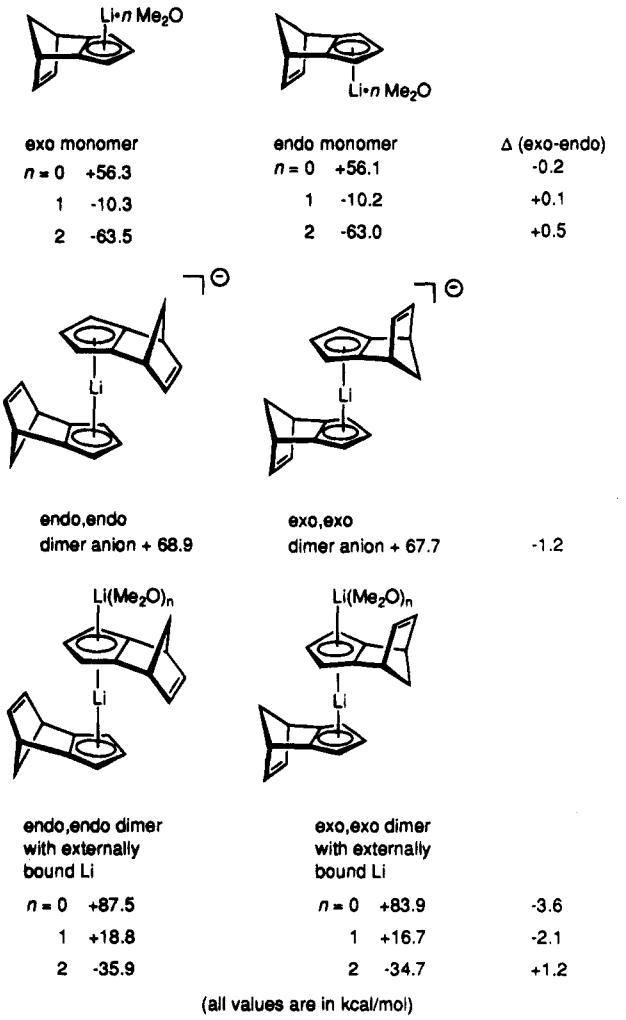

(26) (a) Bauer, W.; Müller, G.; Pi, R.; Schleyer, P. v. R. *Angew. Chem.* **1986**, *98*, 1130. *Angew. Chem., Int. Ed. Engl.* **1986**, *25*, 1103. (b) Bauer, W.; Klusener, P. A. A.; Harder, S.; Kanters, J. A.; Duisenberg, A. J. M.; Brandsma, L.; Schleyer, P. v. R. *Organometallics* **1988**, *7*, 552. (c) Gregory, K.; Bremer, M.; Bauer, W.; Schleyer, P. v. R.; Lorenzen, N. P.; Kopf, J.; Weiss, E. *Organometallics* **1990**, *9*, 1485. (d) Hoffmann, D.; Bauer, W.; Schleyer, P. v. R. *J. Chem. Soc., Chem. Commun.* **1990**, 208. (e) Bauer, W.; Schleyer, P. v. R. In *Advances in Carbanion Chemistry;* Snieckus, V., Ed.; Jai Press: Greenwich, CT, 1992; Vol. 1, p 89. (f) Bauer, W.; Schleyer, P. v. R. *Magn. Reson. Chem.* **1988**, *26*, 827. (g) Anders, E.; Opitz, A.; Bauer, W. *Synthesis* **1991**, 1221. (h) Edelmann, F. T.; Knösel, F.; Pauer, F.; Stalke, D.; Bauer, W. *J. Organomet. Chem.* **1992**, *438*, 1. (i) Bauer, W.; Hampel, F. *J. Chem. Soc., Chem. Commun.* **1992**, 903.

(27) (a) Günther, H. *Proceedings of the 10th National Conference on Molecular Spectroscopy with International Participation*; Bulgarian Academy of Sciences: Blagdoevgrad, Bulgaria, 1988. (b) Harder, S.; Boersma, J.; Brandsma, L.; van Mier, G. P. M.; Kanters, J. A. *J. Organomet. Chem.* **1989**, *364*, 1. (c) Moene, W.; Vos, M.; de Kanter, F. J. J.; Klumpp, G. W.; Spek, A. L. *J. Am. Chem. Soc.* **1989**, *111*, 3463. (d) Arnett, E. M.; Fisher, F. J.; Nichols, M. A.; Ribeiro, A. A. *J. Am. Chem Soc.* **1989**, *111*, 748. (e) Arnett, E. M.; Fisher, F. J.; Nichols, M. A.; Ribeiro, A. A. *J. Am. Chem Soc.* **1990**, *112*, 801. (f) Harder, S.; Boersma, J.; Brandsma, L.; Kanters, J. A.; Duisenberg, A. J. M.; van Lenthe, J. H. *Organometallics* **1990**, *9*, 511. (g) Nichols, M. A.; McPhail, A. T.; Arnett, E. M. *J. Am. Chem. Soc.* **1991**, *113*, 6222. (h) Sethson, I.; Johnels, D.; Lejon, T.; Edlund, U.; Wind, B.; Sygula, A.; Rabideau, P. W. *J. Am. Chem. Soc.* **1992**, *114*, 953. (i) Balzer, H.; Berger, S. *Chem. Ber.* **1992**, *125*, 733. (j) DeLong, G. T.; Pannell, D. K.; Clarke, M. T.; Thomas, R. D. *J. Am. Chem. Soc.* **1993**, *115*, 7013. (k) Ahlbrecht, H.; Harbach, J.; Hauck, T.; Kalinowski, H.-O. *Chem. Ber.* **1992**, *125*, 1753. (l) Anders, E.; Opitz, A.; Boese, R. *Chem. Ber.* **1992**, *125*, 1267. (m) Balzer, H.; Berger, S. *Chem. Ber.* **1992**, *125*, 733.

3(23) and isodiCpLi (**6**) both exhibit monomer–dimer equilibria at low temperatures but are exclusively monomeric at rt. However, whereas **6** exhibits a strong exo lithium preference in both aggregates, the lithium is observed to be endo-oriented both in monomeric and in dimeric **3(23)**. Undoubtedly, this must be a consequence of the additional double bond in **3(23)** which is not present in **6**.

MNDO Calculations. Chart 1 shows the MNDO calculated heats of formation for differently solvated monomers and dimers of **3(23)**. Dimethyl ether ($\Delta H°$ = −51.2 kcal/mol)[28] was employed as a model ligand for THF.

The maximum number, n, of ligands was restricted to 2. For n = 3, it was generally found that one ligand is extruded from the molecule by the program.

As can be seen from Chart 1, the MNDO data do not provide a unique picture. The differences in $\Delta H°$ for the corresponding exo/endo pairs of isomers are compara-tively small. In the case of the monomer, the nonsolvated endo monomer is slightly (by 0.2 kcal/mol) more stable than its exo analogue. However, it is unlikely that we would observe an unsolvated endo monomer in THF solution. For the mono- and disolvated species, the exo isomers are slightly more stable than the endo species (by 0.1 and 0.5 kcal/mol, respectively). We believe that in THF solution a (di-)solvated endo monomer is present.

For the dimers, the endo isomer with externally bound lithium and two Me_2O ligands is more stable than the corresponding exo isomer. In the case of isodiCpLi (**6**), the analogous species was deduced[12] to be the prevailing one in THF solution. We assume the same to hold for **3(23)**; i.e., the dimer anion sandwich must be in close contact with the Li^+ counterion as shown in Chart 1. Thus, MNDO confirms the stability of the endo,endo dimer over its exo,exo analogue.

The modest discrepancies concerning the location of lithium between the experiments and MNDO may be attributed (at least in part) to the known overestimation of Li,H interactions by MNDO.[29] Thus, attractive forces between lithium and H10(syn) in the calculated exo monomers [see **3(23)**] might explain the "wrong" MNDO-derived location of lithium with respect to experiment.

The experimentally-determined endo preference of lithium in **3(23)** as compared to its hydrogenated analogue **6** must obviously be ascribed to the presence of the double bond at C8,C9. Thus, it might be argued that additional coordination of lithium by the double bond as in **30** is the driving force for the endo location

30

of lithium. Surprisingly, MNDO calculations show no evidence for this: the distances between lithium and C8 in the nonsolvated monomer, the disolvated monomer, and the endo,endo dimer anion are 3.45, 3.65, and 3.62 Å, respectively. Thus, it appears that additional coordination by the C8,C9 double bond at lithium plays only a minor role.

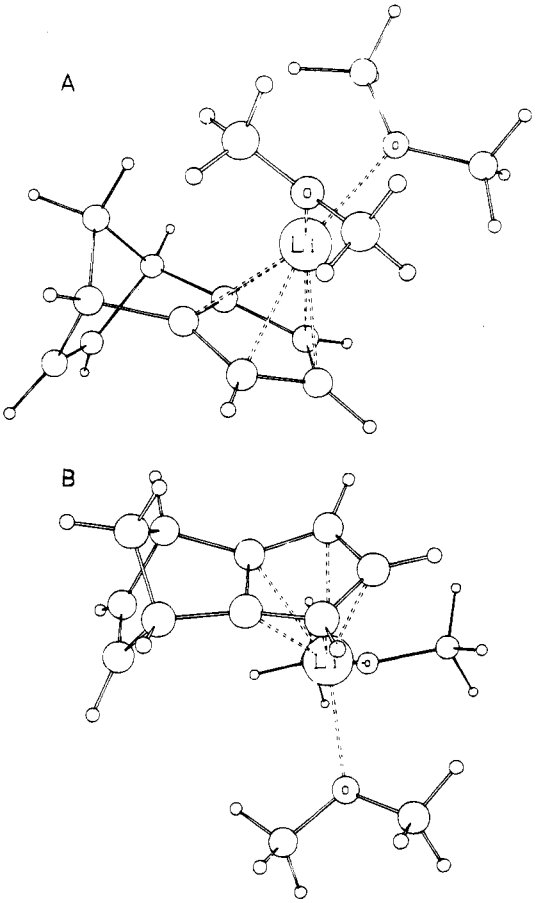

Figure 5. MNDO calculated structure of disolvated exo (A) and endo (B) monomer of **3(23)**.

Figure 5 shows the MNDO calculated structures of disolvated (Me_2O) exo (A) and endo (B) monomer of **3(23)**. Therein, the missing double bond complexation of lithium in the endo isomer (B) becomes obvious.

Mechanistic Implications

Whereas isodiCpLi (**6**) reacts stereospecifically at the endo face at low temperatures (see Introduction), both exo and endo quench products are obtained for **3** under comparable conditions. We have explained[12] the behavior of **6** by assuming that exo,exo dimer **8** is more reactive than exo monomer **9**. Stated differently, the associated activation barrier must be lowered in the dimer. Since in **3** both endo,endo dimer **27** and endo monomer **28** are present in comparable amounts at low temperature, analogous behavior should lead exclusively to exo quench product **5**. Since we observe both **4** *and* **5** as quench products, the implication is the reactivity of dimer **27** must be of comparable to monomer **28**. Hence, in **3**, either dimer **27** must be less reactive than dimer **8** or monomer **28** must be more reactive than monomer **9**.

Conclusions

The stereochemical course of the reaction of lithium tricyclo[5.2.1.0^{2,6}]deca-3,5,8-trienide (**3**) with $BrCH_2CD_2Cl$ proceeds without facial stereoselectivity. The exo

(28) Kaufmann, E.; Gose, J.; Schleyer, P. v. R. *Organometallics* **1989**, *8*, 2577.
(29) Kaufmann, E.; Raghavachari, K.; Reed, A.; Schleyer, P. v. R. *Organometallics* **1988**, *7*, 1597. Also see for the description of an improved semi-empirical method: Anders, E.; Koch, R.; Freunscht, P. *J. Comp. Chem.* **1993**, *14*, 1301.

product predominates only slightly with chlorotrimethylsilane as electrophile. With $FeCl_2$, **3** is transformed into the ferrocenes **20-22**, with the exo/exo isomer being favored (56%) over the exo/endo (38%) and endo/endo counterparts (6%). Thus, a considerable damping effect on the stereoselectivity of electrophile capture is observed experimentally with **3** relative to its dihydro derivative **6** whose exo face is attacked preferentially.

Multinuclear NMR spectroscopy has demonstrated that lithium salt **3** consists of a 0.7:1 molar mixture of endo,endo dimer **27** and endo monomer **28** in 1 M THF solution at −109 °C. At +26 °C, monomer **28** is present exclusively or nearly so. The endo site of the lithium cations in **27** and in **28** is opposite the exo preferences found for monomeric as well as dimeric isodiCpLi (**6**) under similar conditions. The lithium location in **3** was ascertained by the ^6Li, ^1H HOESY technique, as well as by interpretation of the ^1H, ^{13}C, and ^6Li chemical shift data. High-field chemical shifts in the ^6Li spectrum (δ = −7.12 for monomer **28** and δ = −11.68 for sandwiched lithium in dimeric **27**) are similar to earlier observations made for isodiCpLi (**6**),[12] camphor-derived CCpLi (**24**),[13a] and verbenone-derived VCpLi (**29**).[13b] MNDO calculations do show an increased stability for the endo isomer of **3** but find the exo lithium monomer of **3** to be slightly more stable than its endo counterpart. This modest error may be interpreted as a consequence of the known MNDO overestimation of Li,H interactions. The endo,endo dimer of **3** is computed by MNDO to be more stable than the exo,exo isomer, in agreement with the experimental findings. The results of electrophilic capture experiments (quench reactions with CH_3I) between isodiCpLi **6** and **3** suggest either that dimeric **6** is *more* reactive than dimeric **3** or that monomeric **6** is *less* reactive than monomeric **3**.

Experimental Section

NMR spectra on **3** were recorded on a JEOL GX400 spectrometer under conditions described previously.[12,13,25] A 1 M solution of **3**(**23**) (enriched 96% with ^6Li) in THF-d_8 in a 5 mm tube was employed. Selected parameters of the spectra shown in this paper are as follows:

Figure 1 (1D-ROE difference spectrum): T = +26 °C, pulse sequence (1), spin lock time 0.7 s, selective 5 mm ^1H probehead, 90° pulse width (attenuated) = 44 μs, acquisition time 3.0 s, relaxation delay 2.4 s, selective 180° pulse width 14 ms, 64 scans per irradiation point, measurement time 1 h.

Figure 2 (phase-sensitive ^{13}C, ^1H HOESY spectrum): T = +26 °C, pulse sequence (3), ^1H, ^{13}C dual probehead, mixing time 1.7 s, 8 loops through evolution and mixing period before acquisition, 512 complex data points in t_2, 56 increments in t_1, zero-filled to 256 hypercomplex data points, spectral widths 13774 Hz (f_2) and 2270 Hz (f_1), Gaussian apodization in f_1 and f_2, measurement time 15 h.

Figure 3 (phase-sensitive ^6Li, ^1H HOESY spectrum): T = +26 °C, pulse sequence (2) without decoupling during t_2, mixing time 2.0 s, 10 mm multinuclear probehead, spectral widths 400 Hz (f_2) and 2770 Hz (f_1), 256 complex points in t_2, 128 increments in t_1, zero-filled to 512 hypercomplex data points in t_1, 32 scans per t_1 increment, relaxation delay 2.6 s, Gaussian apodization in t_1 and t_2, measurement time 12.5 h.

Figure 4 (magnitude mode ^6Li, ^1H HOESY spectrum): T = −108 °C, nonspinning sample, pulse sequence (2) without decoupling during t_2, mixing time 2.0 sec, 10 mm multinuclear probehead, spectral widths 1000 Hz (f_2) and 2770 Hz (f_1), 512 complex data points in t_2, 128 increments in t_1, zero-filled to 256 complex data points in t_1, 32 scans per t_1 increment, relaxation delay 2.5 s, Gaussian apodization in t_1 and t_2, measurement time 6 h.

MNDO calculations were carried out on a CONVEX C220 computer and on a Silicon Graphics Indigo workstation by using the VAMP4 (vectorized AMPAC) program. The keyword EF (eigenvector following) was employed for the structure optimization. No symmetry constraints were imposed. The Li parameters were those provided by Clark and Thiel.[30]

Spirocyclopropanation of 3. Lithium salt **3** (500 mg, 3.67 mmol) was dissolved in THF (25 mL), and the clear solution was cooled to 0 °C. A solution of 1-bromo-2-chloroethane-2-d_2 (1.07 g, 7.35 mmol) in 10 mL of THF was slowly introduced via cannula over 10 min. The mixture was stirred at 0 °C for 1 h, cooled to −78 °C, treated slowly with lithium bis(trimethylsilyl)amide (9.3 mL, 1.0 M in THF, 9.18 mmol) via syringe, stirred at −78 °C for 2 h, and allowed to warm to room temperature. After 10 h, water (50 mL) was added and the mixture was poured into ether (50 mL). The layers were separated and the aqueous phase was extracted with ether (3 × 30 mL). The combined ethereal layers were dried, filtered, and concentrated to give 360 mg (62%) of an approximately 50:50 mixture of **10** and **11** (^1H NMR): ^1H NMR (300 MHz, C_6D_6) δ 6.27 (t, J = 1.7 Hz, 2 H), 5.32 (s, 2 H), 3.38 (t, J = 1.7 Hz, 2 H), 2.17 (dt, J = 7.6, 1.7 Hz, 1 H), 2.03 (dt, J = 7.6, 1.7 Hz, 1 H), 0.08 (s, 2 H for **11**), 0.04 (s, 2 H for **10**); ^{13}C NMR (75 MHz, C_6D_6) ppm 151.5, 138.8, 122.2, 59.8, 44.4, 39.8, 2.6, 1.4; MS m/z (M^+) calcd 158.1064, obsd 158.1056.

Diels−Alder Cycloaddition to 10 and 11. The mixture of **10** and **11** was dissolved in benzene (50 mL). *N*-Phenylmaleimide (383 mg, 2.2 mmol) was added, and the mixture was stirred at rt for 24 h and concentrated to leave a light yellow oil. The oil was placed atop a short column of kieselghur and eluted with 10% ethyl acetate in petroleum ether to give 491 mg (67%) of **12/13** as a white crystalline solid: mp 175−176 °C (from ethyl acetate); IR ($CHCl_3$, cm^{-1}) 1712; ^1H NMR (300 MHz, $CDCl_3$) δ 7.45 (t, J = 7.4 Hz, 2 H), 7.37 (d, J = 7. Hz, 1 H), 7.25 (d, J = 7.4 Hz, 2 H), 6.59 (s, 2 H), 2.94 (s, 2 H), 2.46 (s, 2 H), 2.26 (d, J = 6.4 Hz, 1 H), 2.12 (d, J = 6.4 Hz, 1 H), 0.62 (s, 2 H for **13**), 0.53 (s, 2 H for **12**); ^2H NMR (46 MHz, $CDCl_3$) δ 0.56 (br d, 4 D); ^{13}C NMR (75 MHz, $CDCl_3$) ppm 177.4, 161.4, 139.3, 132.1, 129.1, 128.4, 126.1, 70.0, 51.9, 49.2, 46.9, 39.1, 7.9, 2.6; MS m/z (M^+) calcd 331.1542, obsd 331.1543.

***exo*- and *endo*-Tricyclo[5.2.1.0^{2,6}]deca-2,5,8-trienyltrimethylsilane (14/15).** A solution of **1** (2.20 g, 16.9 mmol) in hexane (20 mL) and ether (20 mL) was cooled to 0 °C, *n*-butyllithium (14.1 mL, 16.9 mmol, 1.2 M in hexane) was added slowly via syringe over 10 min, and the mixture was stirred at rt for 10 h, cooled to −78 °C, and diluted with 50 mL of THF. After the solid had dissolved, a solution of chlorotrimethylsilane (3.67 g, 33.8 mmol) in 10 mL of dry THF was introduced via cannula and stirring was maintained for 2 h at −78 °C and at rt for 6 h. Ether (100 mL) was added, the mixture was poured into water (100 mL), and the aqueous layer was extracted with ether (3 × 100 mL). The combined organic layers were washed with brine (100 mL), dried, and evaporated to leave an oil that was purified by preparative HPLC (petroleum ether, 12 recycles) with **14** (1.57 g, 46%) eluting before **15** (1.43 g, 42%).

Data for **14**: mp 50−51.4 °C (from pentane); IR (CCl_4, cm^{-1}) 1309, 1253, 1013, 933, 870, 845, 827; ^1H NMR (300 MHz, C_6D_6) δ 6.29 (t, J = 1.7 Hz, 2 H), 5.83 (d, J = 1.1 Hz, 2 H), 3.38 (t, J = 1.7 Hz, 2 H), 3.34 (m, J = 1.3 Hz, 1 H), 2.23 (m, 1 H), 2.11 (d, J = 7.8 Hz, 1 H), −0.08 (s, 9 H); ^{13}C NMR (75 MHz, C_6D_6) ppm 154.8, 140.2, 117.1, 61.3, 53.9, 44.6, −1.9; MS m/z (M^+) calcd 202.1177, obsd 202.1180.

Data for **15**: IR (neat, cm^{-1}) 1250, 842; ^1H NMR (300 MHz, C_6D_6) δ 6.34 (t, J = 1.6 Hz, 2 H), 5.79 (d, J = 0.9 Hz, 2 H), 3.40 (t, J = 1.5 Hz, 2 H), 3.30 (br s, 1 H), 2.24 (d, J = 7.4 Hz,

(30) Thiel, W.; Clark, T. Unpublished (see the MNDOC program: Thiel, W. *QCPE No., 438*).

1 H) 2.05 (d, J = 7.4 Hz, 1 H), −0.05 (s, 9 H); ^{13}C NMR (62.5 MHz, C_6D_6) ppm 154.6, 139.2, 116.2, 62.8, 53.6, 44.6, −2.1; MS m/z (M^+) calcd 202.1144, obsd 202.1161.

Diels–Alder Addition to 14. Silane **14** (110 mg, 0.54 mmol), *N*-phenylmaleimide (94 mg, 0.54 mmol), and benzene (50 mL) were combined at rt and stirred for 24 h. The solvent was evaporated, and the residue was placed atop a column of kieselghur and eluted with 10% ethyl acetate in petroleum ether to give **16** (169 mg, 83%) as a white solid: mp 183–184 °C (from ethyl acetate); IR ($CHCl_3$, cm^{-1}) 1710; ^{1}H NMR (300 MHz, $CDCl_3$) δ 7.43 (t, J = 7.8 Hz, 2 H), 7.36 (d, J = 7.2 Hz, 1 H), 7.14 (m, 2 H), 6.36 (br s, 2 H), 5.57 (d, J = 2.8 Hz, 1 H), 3.66 (dd, J = 1.6, 5.3 Hz, 1 H), 3.46 (dd, J = 3.0, 2.0 Hz, 1 H), 3.37 (d, J = 7.9 Hz, 1 H), 3.23 (br s, 2 H), 2.50 (d, J = 9.6 Hz, 1 H), 1.97 (d, J = 9.6 Hz, 1 H), 1.40 (s, 1 H), −0.04 (s, 9 H); ^{13}C NMR (62.5 MHz, $CDCl_3$) ppm 177.6, 176.3, 156.0, 140.4, 139.0, 132.1, 129.1, 128.5, 126.7, 116.2, 72.2, 63.3, 55.1, 52.9, 51.3, 49.7, 45.2, 42.4, 0.1; MS m/z (M^+) calcd 375.1655, obsd 375.1623. Anal. Calcd for $C_{23}H_{25}NO_2Si$: C, 73.56; H, 6.71. Found: C, 73.40; H, 6.79.

Diels–Alder Addition to 15. Silane **15** (280 mg, 1.14 mmol), *N*-phenylmaleimide (197 mg, 1.14 mmol), and benzene (50 mL) were combined at rt, stirred for 24 h, and concentrated. The residue was purified by chromatography to give **17** as the major isomer: 290 mg (68%) of white solid, mp 146.5–147.5 °C (from ethyl acetate); IR ($CHCl_3$, cm^{-1}) 1704; ^{1}H NMR (300 MHz, $CDCl_3$) δ 7.45 (m, 2 H), 7.38 (d, J = 7.2 Hz, 1 H), 7.23 (m, 2 H), 6.56 (t, J = 1.7 Hz, 2 H), 3.50 (s, 2 H), 3.45 (s, 2 H), 2.35 (s, 2 H), 2.26 (dt, J = 5.0, 1.5 Hz, 1 H), 2.08 (d, J = 2.5 Hz, 1 H), 1.12 (s, 1 H), −0.02 (s, 9 H); ^{13}C NMR (75 MHz, $CDCl_3$) ppm 177.5, 161.4, 139.2, 131.9, 129.1, 128.5, 126.3 70.0, 49.7, 48.5, 46.9, 42.8, −0.3; MS m/z (M^+) calcd 375.1655, obsd 375.1668. Anal. Calcd for $C_{23}H_{25}NO_2Si$: C, 73.56; H, 6.71. Found: C, 73.77; H, 6.70.

(η^5-*exo*-Tricyclo[5.2.1.0^{2,6}]deca-2,5,8-trien-3-yl)trichlorotitanium (18). Silane **14** (1.80 g, 8.9 mmol) dissolved in 25 mL of toluene was added via cannula over 20 min to a cold (−78 °C) solution of titanium tetrachloride (1.69 g, 8.9 mmol) in 50 mL of toluene. The deep red solution was stirred at −78 °C for 2 h, warmed to rt, and concentrated *in vacuo* after 10 h to give a black-red residue. Toluene (50 mL) was added, the mixture was filtered, and the filtrate was concentrated *in vacuo*. A portion of the residue was sublimed (95 °C, 0.003 Torr) to afford 1.32 g (52%) of **18** as a red microcrystalline product. The remaining material was recrystallized to produce an additional 0.53 g (21%) of the complex: mp 122–123 °C; ^{1}H NMR (300 MHz, $CDCl_3$) δ 7.11 (t, J = 3 Hz, 1 H), 6.80 (dd, J = 2 Hz, 2 H), 6.52 (d, J = 3 Hz, 2 H), 4.12 (dddd, J = 2, 2, 1.5, 1.5 Hz, 2 H), 2.54 (br m, 2 H); ^{13}C NMR (75 MHz, $CDCl_3$) ppm 158.9, 144.5, 126.0, 115.3, 67.8, 47.8; MS m/z (M^+) calcd 283.9219, obsd 283.9201. Anal. Calcd for $C_{10}H_9Cl_3Ti$: C, 42.38; H, 3.20. Found: C, 42.62; H, 3.24.

(η^5-*exo*-Tricyclo[5.2.1.0^{2,6}]deca-2,5,8-trien-3-yl)(η^5-methylcyclopentadienyl)dichlorotitanium (19). A solution of methylcyclopentadienyllithium (30.4 mg, 0.35 mmol) in 30 mL of THF was cooled to 0 °C and added via cannula to a cold (0 °C) solution of **18** (100 mg, 0.35 mmol) in 30 mL of THF. After the addition was complete, the mixture was stirred for 2 h at 0 °C and at rt for 2 h before being concentrated *in vacuo*. The residue was taken up in CH_2Cl_2 (50 mL), passed through a 1-in. pad of Celite, and concentrated to give a semisolid which was sublimed (145 °C, 0.003 Torr) to give **19** as a red crystalline solid: mp 157–158 °C (76 mg, 66%); ^{1}H NMR (300 MHz, $CDCl_3$) δ 6.68 (t, J = 1.8 Hz, 1 H), 6.39 (t, J = 2.8 Hz, 1 H), 6.38 (t, J = 2.6 Hz, 2 H), 6.30 (t, J = 2.6 Hz, 2 H), 6.21 (m, 3 H), 3.83 (t, J = 1.6 Hz, 1 H), 2.38 (s, 2 H), 2.34 (s, 3 H), 2.04 (dd, J_{AB} = 70.13 Hz, 1 H); ^{13}C NMR (62.5 MHz, $CDCl_3$) ppm 152.8, 143.6, 134.6, 133.9, 123.4, 123.2, 115.4, 113.7, 109.1, 65.8, 47.2, 16.4; MS m/z (M^+) calcd 328.0079, obsd 328.0068.

Bis(η^5-tricyclo[5.2.1.0^{2,6}]deca-2,5,8-trien-6-yl)iron (20). A solution of **3** (500 mg, 3.67 mmol) in THF (25 mL) was added slowly via cannula during 1 h to iron(II) chloride (239 mg, 1.88 mmol) slurried in 50 mL of THF at −78 °C. The mixture was warmed to rt and evaporated after 24 h. The residue was taken up in benzene, filtered through a pad of Celite, and concentrated to leave an orange oil. Product distribution was established at this point by ^{1}H NMR. Hexane was added to redissolve the oil. Crystallization at −20 °C gave pure **20** (269 mg, 46%). Comparison of the product isolated with that which remained indicated that the exo,exo compound constituted 56% of the product mixture whereby 38% and 6% of the mixture were the exo,endo and endo,endo products, respectively. Data for **20**: mp 162–163 °C (lit.[16] mp 162.5–163.5 °C); ^{1}H NMR (300 MHz, C_6D_6) δ 6.32 (t, J = 1.7 Hz, 4 H), 3.93 (t, J = 2.0 HZ, 4 H), 3.77 (d, J = 2.0 Hz, 2 H), 3.27 (t, J = 1.6 Hz, 4 H), 2.93 (d, J = 6.6 Hz, 2 H), 2.19 (d, J = 6.6 Hz, 2 H); ^{13}C NMR (75 MHz, C_6D_6) ppm 140.9, 104.9, 67.9, 65.8, 61.8, 43.8.

Acknowledgment. Financial support from the National Institutes of Health (Grant CA-12115) and the National Science Foundation (to Ohio State), as well as the Deutsche Forschungsgemeinschaft, the Fonds der Chemischen Industrie, and the Stiftung Volkswagenwerk (to Erlangen) is gratefully acknowledged. M.R.S. thanks the U.S. Department of Education for National Need Fellowships and the Amoco Oil Co. for an Amoco Foundation Fellowship. T. Clark kindly provided the VAMP4 program.

OM940346G